

# Observation of $B^+ \rightarrow \rho^+ \rho^0$

J. Zhang,<sup>48</sup> M. Nakao,<sup>8</sup> K. Abe,<sup>8</sup> K. Abe,<sup>41</sup> T. Abe,<sup>42</sup> I. Adachi,<sup>8</sup> H. Aihara,<sup>43</sup> M. Akatsu,<sup>22</sup> Y. Asano,<sup>48</sup> T. Aso,<sup>47</sup>  
V. Aulchenko,<sup>2</sup> T. Aushev,<sup>12</sup> S. Bahinipati,<sup>5</sup> A. M. Bakich,<sup>38</sup> Y. Ban,<sup>33</sup> E. Banas,<sup>27</sup> P. K. Behera,<sup>49</sup> I. Bizjak,<sup>13</sup>  
A. Bondar,<sup>2</sup> A. Bozek,<sup>27</sup> M. Bračko,<sup>20,13</sup> T. E. Browder,<sup>7</sup> B. C. K. Casey,<sup>7</sup> P. Chang,<sup>26</sup> Y. Chao,<sup>26</sup> B. G. Cheon,<sup>37</sup>  
R. Chistov,<sup>12</sup> S.-K. Choi,<sup>6</sup> Y. Choi,<sup>37</sup> Y. K. Choi,<sup>37</sup> M. Danilov,<sup>12</sup> L. Y. Dong,<sup>10</sup> J. Dragic,<sup>21</sup> A. Drutskoy,<sup>12</sup>  
S. Eidelman,<sup>2</sup> V. Eiges,<sup>12</sup> Y. Enari,<sup>22</sup> C. Fukunaga,<sup>45</sup> N. Gabyshev,<sup>8</sup> A. Garmash,<sup>2,8</sup> T. Gershon,<sup>8</sup> A. Gordon,<sup>21</sup>  
R. Guo,<sup>24</sup> F. Handa,<sup>42</sup> T. Hara,<sup>31</sup> N. C. Hastings,<sup>8</sup> H. Hayashii,<sup>23</sup> M. Hazumi,<sup>8</sup> L. Hinz,<sup>18</sup> T. Hokuue,<sup>22</sup>  
Y. Hoshi,<sup>41</sup> W.-S. Hou,<sup>26</sup> Y. B. Hsiung,<sup>26,\*</sup> H.-C. Huang,<sup>26</sup> Y. Igarashi,<sup>8</sup> T. Iijima,<sup>22</sup> K. Inami,<sup>22</sup> A. Ishikawa,<sup>22</sup>  
R. Itoh,<sup>8</sup> H. Iwasaki,<sup>8</sup> M. Iwasaki,<sup>43</sup> Y. Iwasaki,<sup>8</sup> H. K. Jang,<sup>36</sup> J. H. Kang,<sup>52</sup> J. S. Kang,<sup>15</sup> S. U. Kataoka,<sup>23</sup>  
N. Katayama,<sup>8</sup> H. Kawai,<sup>3</sup> N. Kawamura,<sup>1</sup> T. Kawasaki,<sup>29</sup> D. W. Kim,<sup>37</sup> H. J. Kim,<sup>52</sup> Hyunwoo Kim,<sup>15</sup>  
J. H. Kim,<sup>37</sup> S. K. Kim,<sup>36</sup> K. Kinoshita,<sup>5</sup> P. Koppenburg,<sup>8</sup> S. Korpar,<sup>20,13</sup> P. Krizan,<sup>19,13</sup> P. Krokovny,<sup>2</sup>  
R. Kulasiri,<sup>5</sup> S. Kumar,<sup>32</sup> A. Kuzmin,<sup>2</sup> Y.-J. Kwon,<sup>52</sup> G. Leder,<sup>11</sup> S. H. Lee,<sup>36</sup> T. Lesiak,<sup>27</sup> J. Li,<sup>35</sup> A. Limosani,<sup>21</sup>  
S.-W. Lin,<sup>26</sup> D. Liventsev,<sup>12</sup> J. MacNaughton,<sup>11</sup> G. Majumder,<sup>39</sup> F. Mandl,<sup>11</sup> D. Marlow,<sup>34</sup> H. Matsumoto,<sup>29</sup>  
T. Matsumoto,<sup>45</sup> A. Matyja,<sup>27</sup> W. Mitaroff,<sup>11</sup> K. Miyabayashi,<sup>23</sup> H. Miyata,<sup>29</sup> D. Mohapatra,<sup>50</sup> T. Mori,<sup>4</sup>  
T. Nagamine,<sup>42</sup> Y. Nagasaka,<sup>9</sup> T. Nakadaira,<sup>43</sup> E. Nakano,<sup>30</sup> J. W. Nam,<sup>37</sup> Z. Natkaniec,<sup>27</sup> S. Nishida,<sup>16</sup>  
O. Nitoh,<sup>46</sup> T. Nozaki,<sup>8</sup> S. Ogawa,<sup>40</sup> T. Ohshima,<sup>22</sup> T. Okabe,<sup>22</sup> S. Okuno,<sup>14</sup> S. L. Olsen,<sup>7</sup> W. Ostrowicz,<sup>27</sup>  
H. Ozaki,<sup>8</sup> H. Park,<sup>17</sup> K. S. Park,<sup>37</sup> N. Parslow,<sup>38</sup> J.-P. Perroud,<sup>18</sup> L. E. Piilonen,<sup>50</sup> M. Rozanska,<sup>27</sup> H. Sagawa,<sup>8</sup>  
S. Saitoh,<sup>8</sup> Y. Sakai,<sup>8</sup> T. R. Sarangi,<sup>49</sup> A. Satpathy,<sup>8,5</sup> O. Schneider,<sup>18</sup> J. Schümann,<sup>26</sup> C. Schwanda,<sup>8,11</sup>  
A. J. Schwartz,<sup>5</sup> S. Semenov,<sup>12</sup> K. Senyo,<sup>22</sup> R. Seuster,<sup>7</sup> M. E. Sevier,<sup>21</sup> T. Shibata,<sup>29</sup> H. Shibuya,<sup>40</sup> V. Sidorov,<sup>2</sup>  
J. B. Singh,<sup>32</sup> S. Stanić,<sup>8,†</sup> M. Starić,<sup>13</sup> A. Sugi,<sup>22</sup> K. Sumisawa,<sup>8</sup> T. Sumiyoshi,<sup>45</sup> S. Suzuki,<sup>51</sup> S. Y. Suzuki,<sup>8</sup>  
S. K. Swain,<sup>7</sup> T. Takahashi,<sup>30</sup> F. Takasaki,<sup>8</sup> K. Tamai,<sup>8</sup> N. Tamura,<sup>29</sup> M. Tanaka,<sup>8</sup> G. N. Taylor,<sup>21</sup>  
Y. Teramoto,<sup>30</sup> T. Tomura,<sup>43</sup> S. N. Tovey,<sup>21</sup> K. Trabelsi,<sup>7</sup> T. Tsuboyama,<sup>8</sup> T. Tsukamoto,<sup>8</sup> S. Uehara,<sup>8</sup>  
S. Uno,<sup>8</sup> G. Varner,<sup>7</sup> K. E. Varvell,<sup>38</sup> C. C. Wang,<sup>26</sup> C. H. Wang,<sup>25</sup> J. G. Wang,<sup>50</sup> M.-Z. Wang,<sup>26</sup>  
Y. Watanabe,<sup>44</sup> E. Won,<sup>15</sup> B. D. Yabsley,<sup>50</sup> Y. Yamada,<sup>8</sup> A. Yamaguchi,<sup>42</sup> Y. Yamashita,<sup>28</sup> M. Yamauchi,<sup>8</sup>  
H. Yanai,<sup>29</sup> Heyoung Yang,<sup>36</sup> Y. Yusa,<sup>42</sup> Z. P. Zhang,<sup>35</sup> Y. Zheng,<sup>7</sup> V. Zhilich,<sup>2</sup> D. Žontar,<sup>19,13</sup> and D. Zürcher<sup>18</sup>

(The Belle Collaboration)

<sup>1</sup>Aomori University, Aomori

<sup>2</sup>Budker Institute of Nuclear Physics, Novosibirsk

<sup>3</sup>Chiba University, Chiba

<sup>4</sup>Chuo University, Tokyo

<sup>5</sup>University of Cincinnati, Cincinnati, Ohio 45221

<sup>6</sup>Gyeongsang National University, Chinju

<sup>7</sup>University of Hawaii, Honolulu, Hawaii 96822

<sup>8</sup>High Energy Accelerator Research Organization (KEK), Tsukuba

<sup>9</sup>Hiroshima Institute of Technology, Hiroshima

<sup>10</sup>Institute of High Energy Physics, Chinese Academy of Sciences, Beijing

<sup>11</sup>Institute of High Energy Physics, Vienna

<sup>12</sup>Institute for Theoretical and Experimental Physics, Moscow

<sup>13</sup>J. Stefan Institute, Ljubljana

<sup>14</sup>Kanagawa University, Yokohama

<sup>15</sup>Korea University, Seoul

<sup>16</sup>Kyoto University, Kyoto

<sup>17</sup>Kyungpook National University, Taegu

<sup>18</sup>Institut de Physique des Hautes Énergies, Université de Lausanne, Lausanne

<sup>19</sup>University of Ljubljana, Ljubljana

<sup>20</sup>University of Maribor, Maribor

<sup>21</sup>University of Melbourne, Victoria

<sup>22</sup>Nagoya University, Nagoya

<sup>23</sup>Nara Women's University, Nara

<sup>24</sup>National Kaohsiung Normal University, Kaohsiung

<sup>25</sup>National Lien-Ho Institute of Technology, Miao Li

<sup>26</sup>Department of Physics, National Taiwan University, Taipei

<sup>27</sup>H. Niewodniczanski Institute of Nuclear Physics, Krakow

<sup>28</sup>Nihon Dental College, Niigata

<sup>29</sup>Niigata University, Niigata

<sup>30</sup>Osaka City University, Osaka

- <sup>31</sup>Osaka University, Osaka  
<sup>32</sup>Panjab University, Chandigarh  
<sup>33</sup>Peking University, Beijing  
<sup>34</sup>Princeton University, Princeton, New Jersey 08545  
<sup>35</sup>University of Science and Technology of China, Hefei  
<sup>36</sup>Seoul National University, Seoul  
<sup>37</sup>Sungkyunkwan University, Suwon  
<sup>38</sup>University of Sydney, Sydney NSW  
<sup>39</sup>Tata Institute of Fundamental Research, Bombay  
<sup>40</sup>Toho University, Funabashi  
<sup>41</sup>Tohoku Gakuin University, Tagajo  
<sup>42</sup>Tohoku University, Sendai  
<sup>43</sup>Department of Physics, University of Tokyo, Tokyo  
<sup>44</sup>Tokyo Institute of Technology, Tokyo  
<sup>45</sup>Tokyo Metropolitan University, Tokyo  
<sup>46</sup>Tokyo University of Agriculture and Technology, Tokyo  
<sup>47</sup>Toyama National College of Maritime Technology, Toyama  
<sup>48</sup>University of Tsukuba, Tsukuba  
<sup>49</sup>Utkal University, Bhubaneswar  
<sup>50</sup>Virginia Polytechnic Institute and State University, Blacksburg, Virginia 24061  
<sup>51</sup>Yokkaichi University, Yokkaichi  
<sup>52</sup>Yonsei University, Seoul

We report the first observation of the charmless vector-vector decay process  $B^+ \rightarrow \rho^+ \rho^0$ . The measurement uses a  $78 \text{ fb}^{-1}$  data sample collected with the Belle detector at the KEKB asymmetric  $e^+e^-$  collider operating at the  $\Upsilon(4S)$  resonance. We obtain a branching fraction of  $\mathcal{B}(B^+ \rightarrow \rho^+ \rho^0) = (31.7 \pm 7.1(\text{stat.})^{+3.8}_{-6.7}(\text{sys.})) \times 10^{-6}$ . An analysis of the  $\rho$  helicity-angle distributions gives a longitudinal polarization of  $\Gamma_L/\Gamma = (94.8 \pm 10.6(\text{stat.}) \pm 2.1(\text{sys.}))\%$ .

PACS numbers: 13.25.Hw, 14.40.Nd

Charmless  $B$  meson decays to two pseudoscalar mesons (PP) or to pseudoscalar plus vector meson (PV) final states have been studied in some detail [1]. However, measurements of decays to charmless vector-vector (VV) final states are rather limited; to date only  $B \rightarrow \phi K^*$  decays have been observed [2]. The VV decays provide opportunities to search for direct- $CP$  and/or  $T$  violations through angular correlations between the vector meson decay final states [3, 4]. In  $B^+ \rightarrow \rho^+ \rho^0$  decays, isospin-breaking processes such as electroweak penguins [5] or  $\rho^0$ - $\omega$  interference [6, 7], which may produce a sizable direct- $CP$ -violating asymmetry, are expected to be enhanced relative to  $CP$ -conserving processes such as gluonic penguins, which are nominally forbidden by isospin symmetry. The branching fraction for this process is predicted to be  $\mathcal{O}(10^{-5})$  [7, 8].

In this paper, we present the first observation of the VV decay mode  $B^+ \rightarrow \rho^+ \rho^0$  [9]. These decays produce final states where both  $\rho$  mesons are either longitudinally or transversely polarized. We denote the corresponding amplitudes as  $H_{00}$  and  $H_{11}$ , respectively.

The analysis is based on a  $78 \text{ fb}^{-1}$  data sample containing  $85 \times 10^6$   $B$  meson pairs collected at the  $\Upsilon(4S)$  resonance with the Belle detector at the KEKB asymmetric-energy  $e^+e^-$  collider. We also use an off-resonance data sample of  $8.3 \text{ fb}^{-1}$  collected at a center-of-mass energy that is 60 MeV below the  $\Upsilon(4S)$  resonance.

The Belle detector is a large-solid-angle magnetic spec-

trometer. Charged particle tracking is provided by a three-layer silicon vertex detector and a 50-layer central drift chamber (CDC). Charged hadron identification is provided by  $dE/dx$  measurements in the CDC, and arrays of aerogel threshold Čerenkov counters (ACC) and time-of-flight scintillation counters (TOF) that surround the CDC. An electromagnetic calorimeter comprised of CsI(Tl) crystals (ECL) provides photon detection and electron identification. All of these devices are located inside a superconducting solenoidal coil that provides a 1.5 T magnetic field. An iron flux-return located outside of the coil is instrumented to detect  $K_L^0$  mesons and muons. The detector is described in detail elsewhere [10].

We select  $B^+ \rightarrow \rho^+ \rho^0$  candidate events by combining three charged pions and one neutral pion. We require that each charged track has a transverse momentum  $p_t > 0.1 \text{ GeV}/c$ , and is consistent with originating from within  $\delta r < 0.1 \text{ cm}$  in the radial direction and  $|\delta z| < 5 \text{ cm}$  in the electron beam direction of the run-by-run-determined interaction point. We also require that the three charged tracks be positively identified as pions by the CDC, ACC and TOF systems.

Candidate  $\pi^0$  mesons are reconstructed from pairs of photons with an invariant mass in the range  $0.118 \text{ GeV}/c^2 < M(\gamma\gamma) < 0.150 \text{ GeV}/c^2$ . For the ECL barrel region ( $32.2^\circ < \theta < 128.7^\circ$ ), photon energies greater than 50 MeV are required; for the ECL endcap region ( $17.0^\circ < \theta < 31.4^\circ$  or  $130.7^\circ < \theta < 150.0^\circ$ ), this

requirement is increased to 100 MeV. In addition, we only accept  $\pi^0$  candidates with a  $\Upsilon(4S)$  center-of-mass system (cms) momentum  $p_{\pi^0} > 0.5 \text{ GeV}/c$ . The  $\pi^0$  candidates are kinematically constrained to the nominal  $\pi^0$  mass.

Candidate  $\rho$  mesons are reconstructed via their  $\rho^0 \rightarrow \pi^+\pi^-$  and  $\rho^+ \rightarrow \pi^+\pi^0$  decays. For both the charged and neutral modes, we require  $0.65 \text{ GeV}/c^2 < M(\pi\pi) < 0.89 \text{ GeV}/c^2$ .

$B^+ \rightarrow \rho^+\rho^0$  decays are identified using the beam-energy constrained mass  $M_{bc} \equiv \sqrt{(E_{\text{beam}})^2 - (p_B)^2}$  and the energy difference  $\Delta E \equiv E_B - E_{\text{beam}}$ , where  $E_{\text{beam}}$  is the cms beam energy, and  $p_B$  and  $E_B$  are the cms momentum and energy, respectively, of the  $B^+ \rightarrow \rho^+\rho^0$  candidates. The  $\Delta E$  distribution has a tail on the lower side caused by incomplete longitudinal containment of electromagnetic showers in the CsI crystals, and the  $\Delta E$  resolution varies slightly depending on the  $\pi^0$  momentum. We select events in the region  $|\Delta E| < 0.4 \text{ GeV}$ ,  $M_{bc} > 5.2 \text{ GeV}/c^2$  with a signal region defined as  $-0.10 \text{ GeV} < \Delta E < 0.06 \text{ GeV}$  and  $5.272 \text{ GeV}/c^2 < M_{bc} < 5.290 \text{ GeV}/c^2$ . The  $\rho \rightarrow \pi\pi$  daughter momentum distributions are helicity-state dependent: for the  $H_{00}$  state, the two pions have an asymmetric momentum distribution where one pion has low momentum (in the range  $0 \sim 1.3 \text{ GeV}/c$ ) while the other has high momentum ( $1.3 \sim 2.8 \text{ GeV}/c$ ); for the  $H_{11}$  state, the two pions tend to have the same momentum. Because of its higher probability for having a low energy pion, the  $H_{00}$  state has a lower reconstruction efficiency and a  $\Delta E$  resolution that is, on average, about 15% broader than that for the  $H_{11}$  state.

There are large backgrounds from  $e^+e^- \rightarrow q\bar{q}$  continuum events ( $q = u, d, s, c$ ), which tend to have a two-jet-like structure. These are suppressed by requiring  $|\cos\theta_{\text{thr}}| < 0.8$ , where  $\theta_{\text{thr}}$  is the angle between the thrust axis of the candidate tracks and that of the remaining tracks in the event. We achieve further suppression by means of a likelihood ratio derived from a Fisher discriminant formed from six modified Fox-Wolfram moments [11] and  $\theta_B$ , the angle between the  $B$  flight direction and the electron beam direction. The combined rejection for continuum events is 98%, with a 65% loss in signal.

Background contributions from  $b \rightarrow c$  processes are investigated with a large sample of Monte Carlo (MC) events, for which no signal-like peak is found in either the  $\Delta E$  or  $M_{bc}$  distributions. Some rare  $B$  decay processes, such as  $B^+ \rightarrow \eta'\rho^+$ ,  $K^{*+}\rho^0$ ,  $\rho^+K^{*0}$  and  $\rho\pi$ , can survive the event selection but are displaced from the signal in  $\Delta E$ . Moreover, these modes have small branching fractions [12] and low reconstruction efficiencies. MC estimates based on measured upper limits for the branching fractions indicate a possible signal-region yield from these rare modes of seven events; this is taken into account in the systematic error determination, as discussed below.

Figure 1 (left) shows the  $\Delta E$  projection of the selected events in the  $5.272 \text{ GeV}/c^2 < M_{bc} < 5.290 \text{ GeV}/c^2$  signal region. The curve shows the results of a binned maximum-likelihood fit with three components: signal, continuum background, and  $B\bar{B}$  background. The signal is represented by the sum of a Gaussian and a ‘‘Crystal Ball’’ line shape (CB) function [13] with parameters determined from an  $H_{00}$  signal MC that is calibrated with  $B^+ \rightarrow \bar{D}^0\pi^+$ ,  $\bar{D}^0 \rightarrow K^+\pi^-\pi^0$  events. A linear function with a slope determined from the off-resonance data is used to represent the continuum background. The  $B\bar{B}$  background contribution is modeled by a smoothed histogram with a shape that is obtained from MC. In the fit, all parameters other than the normalizations are fixed.

The fit gives a signal yield of  $58.7 \pm 13.2$  events. The statistical significance of the signal, defined as  $\sqrt{-2 \ln(\mathcal{L}_0/\mathcal{L}_{\text{max}})}$ , where  $\mathcal{L}_{\text{max}}$  is the likelihood value at the best-fit signal yield and  $\mathcal{L}_0$  is the value with the signal yield fixed to zero, is 5.3.

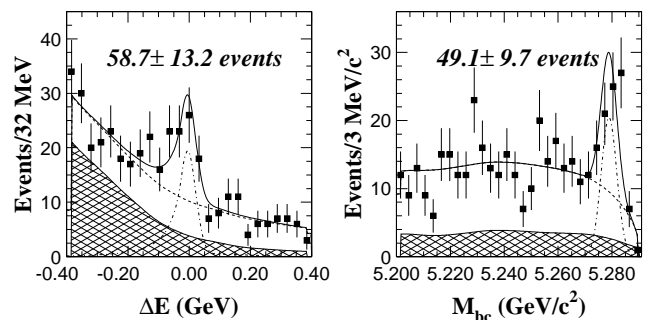


FIG. 1:  $\Delta E$  (left) and  $M_{bc}$  (right) fits to the  $B^+ \rightarrow \rho^+\rho^0$  candidate events. The signal component is shown as a dot-dashed line. The sum of  $B\bar{B}$  and continuum components is shown as a dashed line. The shaded histograms represent the  $B\bar{B}$  background.

Figure 1 (right) shows the  $M_{bc}$  projection of events in the  $-0.10 \text{ GeV} < \Delta E < 0.06 \text{ GeV}$  signal region. The curve shows the results of a binned maximum-likelihood fit that uses a single Gaussian with a MC-determined width to represent the signal, a threshold (ARGUS) function [14] for the continuum background with shape parameters that are determined from the  $\Delta E$  sideband (defined as  $0.1 \text{ GeV} < \Delta E < 0.4 \text{ GeV}$ ), and a smoothed histogram obtained from MC to represent the  $B\bar{B}$  background, normalized according to the MC expectation. This fit gives a signal yield of  $49.1 \pm 9.7$ , with a statistical significance of 6.5.

The fit results and MC efficiencies are summarized in Table I. Since the  $\Delta E$  distribution provides stronger discrimination against rare  $B$ -meson decay backgrounds, we use the  $\Delta E$  fit result for the branching fraction calculation.

Figure 2 shows signal yields extracted from fits to the  $\Delta E$  distributions for different  $M(\pi^+\pi^-)$  and  $M(\pi^+\pi^0)$

TABLE I: Signal yields from the fits to the  $\Delta E$  and  $M_{bc}$  distributions together with the MC-determined efficiencies.

	$\Delta E$ fit	$M_{bc}$ fit
Yield	$58.7 \pm 13.2$ (5.3 $\sigma$ )	$49.1 \pm 9.7$ (6.5 $\sigma$ )
Efficiency $\epsilon_{00}$	2.11%	1.59%
Efficiency $\epsilon_{11}$	3.45%	3.07%

mass bins; the  $\pi\pi$  mass spectra from the signal MC are shown as shaded histograms. The data agree reasonably well with  $B^+ \rightarrow \rho^+ \rho^0$  MC expectations.

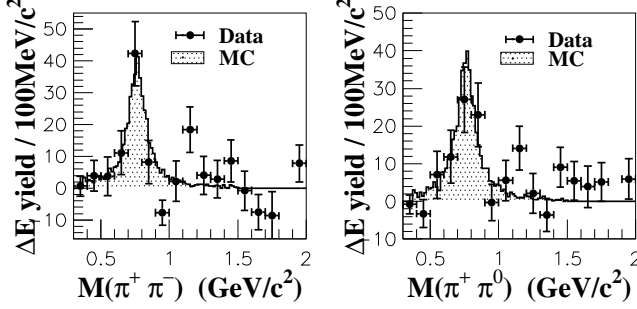


FIG. 2: Data points are the results of fits to the  $\Delta E$  distributions for each  $M(\pi^+\pi^-)$  bin (left) and  $M(\pi^+\pi^0)$  bin (right), where  $D \rightarrow K\pi, \pi\pi, \pi\pi^0$  events are excluded by  $-120 < M(\pi\pi) - M_{D^0} < 30$  MeV/ $c^2$  and  $|M(\pi\pi^0) - M_{D^+}| < 50$  MeV/ $c^2$  vetoes; the histograms are expectations from the signal MC.

We examined the possible contribution from non-resonant processes using MC-generated  $B^+ \rightarrow \pi^+\pi^-\pi^+\pi^0$  events where the final states are distributed uniformly over phase space. After the application of all selection requirements, including the  $\rho$  mass cuts, we find an efficiency that is less than 2% of that for  $B^+ \rightarrow \rho^+\rho^0$  decays. Possible contributions from  $B^+ \rightarrow a_1^+\pi^0$  or  $B^+ \rightarrow a_1^0\pi^+$  decay are examined and found to be smaller than those from non-resonant decays. To account for these contributions, we perform  $\chi^2$  fits to the distributions shown in Fig. 2 with a  $\rho$  plus non-resonant  $\pi\pi$  component included. The resulting non-resonant yield increased by  $1\sigma$  is included in the systematic error.

We use the  $\rho \rightarrow \pi\pi$  helicity-angle ( $\theta_{\text{hel}}$ ) distributions to determine the relative strengths of  $H_{00}$  and  $H_{11}$ . Here  $\theta_{\text{hel}}$  is the angle between the  $\rho$  flight direction in the  $B$  rest frame and  $\pi^+$  flight direction in the  $\rho$  rest frame. The signal yields determined from fits to the  $\Delta E$  distributions for each helicity-angle bin are plotted versus  $\cos\theta_{\text{hel}}$  in Fig. 3 for the  $\rho^0$  (left) and the  $\rho^+$  (right). In determining these yields, bin-by-bin  $H_{00}$ -signal-MC-determined shape parameters are used to extract the signal. We perform a simultaneous  $\chi^2$  fit to the two background-subtracted  $\rho$  helicity-angle distributions using MC-determined expectations for the  $H_{00}$  and  $H_{11}$  helicity states. The

fit results, shown as histograms in Fig. 3, indicate that the longitudinal ( $H_{00}$ ) state dominates. We obtain the acceptance-corrected longitudinal polarization ratio

$$\frac{\Gamma_L}{\Gamma} = (94.8 \pm 10.6(\text{stat.}) \pm 2.1(\text{sys.}))\%,$$

where the systematic error includes uncertainties in the signal yield extraction and the polarization-dependence of the detection efficiency. This dominance of  $H_{00}$  is consistent with theoretical predictions [15].

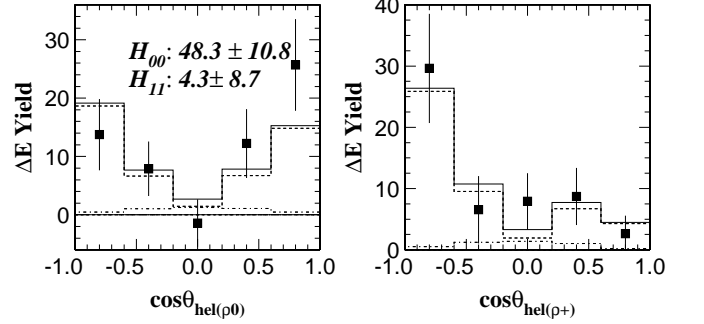


FIG. 3: Data points show the background-subtracted  $\cos\theta_{\text{hel}}$  distributions for the  $\rho^0$  (left) and  $\rho^+$  (right). In each plot the dashed (dot-dashed) histogram is the  $H_{00}$  ( $H_{11}$ ) component of the fit; the solid histogram is their sum. The low yield of events near  $\cos\theta_{\text{hel}(\rho^+)} = 1$  is due to the  $p_{\pi^0} > 0.5$  GeV/ $c$  requirement.

We use MC-determined efficiencies for the two helicity states and the measured polarization ratio to determine the branching fraction. We assign a 3.4% systematic error for tracking that is obtained from a study of partially reconstructed  $D^*$  decays; a 3.6% error for the particle identification efficiency that is based on a study of kinematically selected  $D^{*+} \rightarrow D^0\pi^+, D^0 \rightarrow K^-\pi^+$  decays; a 4.0%  $\pi^0$  reconstruction systematic error that is determined from comparisons of  $\eta \rightarrow \pi^0\pi^0\pi^0$  to  $\eta \rightarrow \pi^+\pi^-\pi^0$  and  $\eta \rightarrow \gamma\gamma$ ; a 5.4% error for continuum suppression that is estimated from a study of  $B^+ \rightarrow \bar{D}^0\pi^+, \bar{D}^0 \rightarrow K^+\pi^-\pi^0$  decays; an error associated with the  $\Delta E$  fit of  ${}^{+7.3}_{-6.7}\%$  that is obtained from changes that occur when each parameter of the fitting functions is varied by  $\pm 1\sigma$ ; a 1% error for the uncertainty in the number of  $B\bar{B}$  events in the data sample; a  ${}^{+0}_{-16.7}\%$  error to account for a possible contribution from non-resonant decays; and a 3.3% error due to uncertainties in the rare  $B$  decay background that is estimated from the change produced by fitting the  $\Delta E$  distribution with the inclusion of an additional component normalized at its MC expectation. We also include a  ${}^{+3.1}_{-6.5}\%$  error due to the uncertainty in the mixture of helicity states that is obtained from the changes in the branching fraction that occur when the longitudinal polarization ratio is lowered by  $1\sigma$  or raised to 100%. The quadratic sum of all of these errors is taken as the total systematic error. We obtain the branching

fraction

$$\mathcal{B}(B^+ \rightarrow \rho^+ \rho^0) = (31.7 \pm 7.1(\text{stat.})_{-6.7}^{+3.8}(\text{sys.})) \times 10^{-6}.$$

As a check, we examined the decay mode  $B^+ \rightarrow \rho^+ \bar{D}^0$ ,  $\bar{D}^0 \rightarrow \pi^+ \pi^-$ , which has the same final state particles as the mode under study, including a  $\pi^0$  with a similar momentum distribution. The same analysis procedure is applied except for an  $|M(\pi\pi) - M_{D^0}| < 13 \text{ MeV}/c^2$  mass selection. For this mode, we obtain a signal yield of  $42.3 \pm 8.5$  events, consistent with MC expectations based on the known branching fraction values [1].

Direct  $CP$  violation would be indicated by a difference in partial rates for  $B^- \rightarrow \rho^- \rho^0$  and  $B^+ \rightarrow \rho^+ \rho^0$ . Separate fits to the  $\Delta E$  distributions find  $29.3 \pm 9.5$   $\rho^- \rho^0$  events and  $29.3 \pm 9.1$   $\rho^+ \rho^0$  events. Since backgrounds from generic  $B\bar{B}$  decays should contribute equally to  $\rho^- \rho^0$  and  $\rho^+ \rho^0$ , we fix the normalizations for  $B\bar{B}$  components at half the value determined from the combined fit.

The charge symmetry of the detector and reconstruction procedure is verified with a sample of  $B^+ \rightarrow \bar{D}^0 \pi^+$ ,  $\bar{D}^0 \rightarrow K^+ \pi^- \pi^0$  decays and their charge conjugates. Here the analysis procedure is similar to that for  $B^+ \rightarrow \rho^+ \rho^0$  but replacing one  $\pi^+$  by a  $K^+$  and the invariant mass requirements by  $|M(K\pi\pi^0) - M_{D^0}| < 50 \text{ MeV}/c^2$ . For these events we find a partial rate asymmetry of  $(-2.1 \pm 2.5)\%$ , which is consistent with zero. We assign 2.5% as the systematic error for the detection and reconstruction asymmetry. The systematic error associated with the  $\Delta E$  fitting procedure is determined to be  $(_{-1.2}^{+0.8})\%$  by shifting each parameter of the fitting functions by  $\pm 1\sigma$  and taking the quadratic sum of the resulting changes in  $\mathcal{A}_{CP}$ . The quadratic sum of these errors is taken as the total systematic error. We obtain the  $CP$  asymmetry

$$\begin{aligned} \mathcal{A}_{CP}(B^\mp \rightarrow \rho^\mp \rho^0) &\equiv \frac{N_{(\rho^- \rho^0)} - N_{(\rho^+ \rho^0)}}{N_{(\rho^- \rho^0)} + N_{(\rho^+ \rho^0)}} \\ &= 0.00 \pm 0.22(\text{stat.}) \pm 0.03(\text{sys.}). \end{aligned}$$

In summary, we have observed the decay  $B^+ \rightarrow \rho^+ \rho^0$  with a statistical significance of 5.3. We measure the branching fraction to be  $\mathcal{B}(B^+ \rightarrow \rho^+ \rho^0) = (31.7 \pm 7.1(\text{stat.})_{-6.7}^{+3.8}(\text{sys.})) \times 10^{-6}$ , where the systematic error includes the error associated with the helicity-mix uncertainty. An analysis of the helicity-angle distributions gives the longitudinal polarization ratio  $\Gamma_L/\Gamma = (94.8 \pm 10.6(\text{stat.}) \pm 2.1(\text{sys.}))\%$ . We also measure  $\mathcal{A}_{CP}(B^\mp \rightarrow \rho^\mp \rho^0) = 0.00 \pm 0.22(\text{stat.}) \pm 0.03(\text{sys.})$ .

We wish to thank the KEKB accelerator group for the excellent operation of the KEKB accelerator. We acknowledge support from the Ministry of Education, Culture, Sports, Science, and Technology of Japan and the Japan Society for the Promotion of Science; the Australian Research Council and the Australian Department of Industry, Science and Resources; National Science Foundation of China under contract No. 10175071; the Department of Science and Technology of India; the BK21 program of the Ministry of Education of Korea and the CHEP SRC program of the Korea Science and Engineering Foundation; the Polish State Committee for Scientific Research under contract No. 2P03B 01324; the Ministry of Science and Technology of Russian Federation; the Ministry of Education, Science and Sport of Slovenia; the National Science Council and the Ministry of Education of Taiwan; and the U.S. Department of Energy.

---

\* on leave from Fermi National Accelerator Laboratory, Batavia, Illinois 60510

† on leave from Nova Gorica Polytechnic, Nova Gorica

- [1] K. Hagiwara *et al.*, Phys. Rev. D **66**, 010001 (2002).
- [2] R. A. Briere *et al.* (CLEO Collaboration), Phys. Rev. Lett. **86**, 3718 (2001); B. Aubert *et al.* (BABAR Collaboration), Phys. Rev. Lett. **87**, 151801 (2001).
- [3] G. Kramer, W.F. Palmer, H. Simma, Nucl. Phys. B **428**, 77 (1994).
- [4] A. Datta, D. London, hep-ph/0303159 (2003).
- [5] D. Atwood, A. Soni, Phys. Rev. D **65**, 073018 (2002).
- [6] S. Gardner, H. B. O'Connell, A. W. Thomas, Phys. Rev. Lett. **80**, 1834-1837 (1998).
- [7] R. Enomoto, M. Tanabashi, Phys. Lett. B **386**, 413 (1996).
- [8] W.S. Hou, K.C. Yang, Phys. Rev. D **61**, 073014 (2000).
- [9] The inclusion of charge conjugate modes is implied unless stated otherwise.
- [10] A. Abashian *et al.* (Belle Collaboration), Nucl. Instr. and Meth. A **479**, 117 (2002).
- [11] G.C. Fox, S. Wolfram, Phys. Lett. B **41**, 1581 (1978); K. Abe *et al.* (Belle Collaboration), Phys. Rev. Lett. **87**, 101801 (2001).
- [12] C.P. Jessop *et al.* (CLEO Collaboration), Phys. Rev. Lett. **85**, 2881 (2000); R. Godang *et al.* (CLEO Collaboration), Phys. Rev. Lett. **88**, 021802 (2002).
- [13] J.E. Gaiser *et al.* (Crystal Ball Collaboration), Phys. Rev. D **34**, 711 (1986).
- [14] H. Albrecht *et al.* (ARGUS Collaboration), Phys. Lett. B **241**, 278 (1990).
- [15] R. Aleksan *et al.*, Phys. Lett. B **356**, 95 (1995).